Progress In Electromagnetics Research, PIER 51, 231–247, 2005

MAGNETIC PROPERTIES OF S-SHAPED SPLIT-RING RESONATORS

H. S. Chen, L. X. Ran, J. T. Huangfu, X. M. Zhang, and K. S. Chen

Electromagnetics Academy
Dept. of Information and Electronic Engineering
Zhejiang University
Hangzhou 310027, China

T. M. Grzegorczyk and J. A. Kong †

Research Laboratory of Electronics
Massachusetts Institute of Technology
Cambridge, MA 02139, USA

Abstract—We present a theoretical analysis of the radiation of an S-shaped split ring resonator (S-SRR) for the realization of a metamaterial exhibiting left-handed properties. It is shown that the structure is resonant due to its internal capacitances and inductances, which can be adjusted such that the electric plasma frequency and magnetic plasma frequency, both due to the S-SRR only, appear within the same frequency band. Using the same idea, we also present some extended S-shaped split-ring resonator structures with improved performance.

† Also with Electromagnetics Academy, Dept. of Information and Electronic Engineering, Zhejiang University, Hangzhou 310027, China

1. INTRODUCTION

Since Pendry et al. [1] proposed, in 1999, the first split-ring resonators (SRR) which exhibits a negative permeability at a given frequency range, multiple modified SRR structures have been reported in the literature [2–5]. A common characteristic of all the SRR used in the realization of metamaterials so far is that they need to be combined with a periodic arrangement of rods in order to exhibit left-handed properties. As a matter of fact, although it is known that the SRR itself does respond to the electric field, the frequencies associated with this response usually does not overlap with the frequency response due to the magnetic field. In Ref [6], Chen et al., proposed an S-shaped SRR structure (S-SRR) which, without the need of additional rods, produces an electric and magnetic response within the same frequency range, thus realizing simultaneously a negative permittivity and a negative permeability, i.e., a left-handed metamaterial [7]. In this paper, we present the theoretical derivation that shows the principles based on which the S-SRR resonates and exhibits a negative permeability as well as a negative permittivity.

2. MAGNETIC PROPERTIES OF S-SRR

A periodic array of S-SRR structures is shown in Fig. 1(a), where each unit cell is composed of two reversed S-shaped metallic strips printed facing each-other. Fig. 1(b) is a sketch of a unit cell in the xz plane, where the solid line indicates the front 'S' pattern, and the dashed line indicates the back 'S' pattern. The dimensions of a unit cell are in the a in the z direction, b in the x direction, and l in the y direction. Thus in the xz plane, $S = ab$ is the area of a periodic unit. The two opposite 'S'-shaped metallic strips generate an '8'-shaped pattern and divide the unit cell into three regions. Based on the geometry of the S-SRR shown in Fig. 1(b), we let F_1 to be the fractional volume of the cell occupied by the top loop of the '8' pattern (Area I, Loop 1), F_2 to be the fractional volume of the cell occupied by the bottom loop of the '8' pattern (Area II, Loop 2), and F_3 to be the fractional volume of the cell not enclosed by the rings (Area III). Based on these definitions we have

$$F_1 + F_2 + F_3 = 1. \tag{1}$$

When a time-varying external field H_0 is applied in the y direction, currents will flow in the split ring. Denoting by I_1 and I_2 the currents in the two loops of the structure, the magnetic fields H_1, H_2 and H_3 in

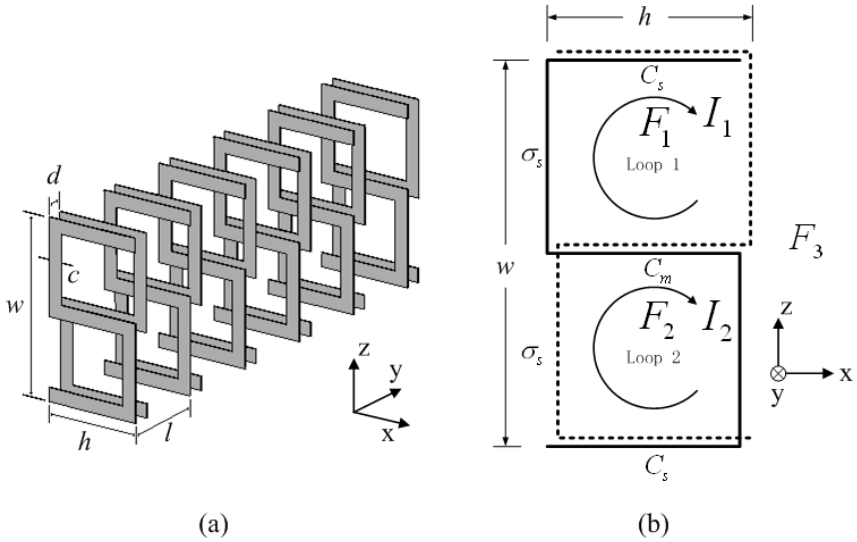

Figure 1. (a) 3-D plot of S-shaped SRR, (b) S-shaped SRR in x-z plane.

the three areas (Area I, Area II, Area III, respectively) should satisfy:

$$\begin{aligned} H_1 - H_2 &= j_1 - j_2 \\ H_1 - H_3 &= j_1 \\ H_1F_1 + H_2F_2 + H_3F_3 &= H_0 \end{aligned} \tag{2}$$

where

$$j_1 = \frac{I_1}{l} \qquad \text{and} \qquad j_2 = \frac{I_2}{l} \tag{3}$$

From the requirements of Equation (2), we can calculate the fields in the three areas:

$$\begin{aligned} H_1 &= H_0 + (1 - F_1)j_1 - F_2j_2 \\ H_2 &= H_0 - F_1j_1 + (1 - F_2)j_2 \\ H_3 &= H_0 - F_1j_1 - F_2j_2 \end{aligned} \tag{4}$$

The units of the currents are Ampere per unit length in the y direction. Note that Equations (2)–(4) are only valid under the assumption that the S-SRRs are sufficiently close to each-other in the y direction, so that the spreading of the magnetic field lines (or fringing effect) can be

neglected. The total electromotive force (emf) around the two loops in one unit cell can be calculated as

$$\begin{aligned} \text{Loop 1}: \ emf_1 &= -\frac{\partial}{\partial t}(\mu_0 H_1 F_1 S) \\ &= \sigma_s I_1 + \frac{1}{C_s}\int I_1 dt + \frac{1}{C_m}\int (I_1 + I_2) dt \qquad (5) \\ \text{Loop 2}: \ emf_2 &= -\frac{\partial}{\partial t}(\mu_0 H_2 F_2 S) \\ &= \sigma_s I_2 + \frac{1}{C_s}\int I_2 dt + \frac{1}{C_m}\int (I_1 + I_2) dt \qquad (6) \end{aligned}$$

where σ_s is the resistance of the metallic strips in each loop, C_m is the capacitance between the center metallic strips, and C_s is the capacitance of the top and bottom metallic strips, as shown in Fig. 1(b). Note that the currents feed into the capacitance of C_m is $I_1 + I_2$, which can be seen from Fig. 1(b). The capacitance between the two metallic strips can be calculated as

$$C_s = C_m = \varepsilon_0 \frac{hc}{d} + \varepsilon_0 \frac{hc}{l-d} \qquad (7)$$

Upon using Equation (4) and replacing $\frac{\partial}{\partial t}$ by $-i\omega$ and $\int dt$ by $\frac{1}{-i\omega}$, Equations (5) and (6) become

$$\begin{aligned} i\omega\mu_0 H_1 F_1 S - \sigma_s j_1 l + \frac{j_1 l}{i\omega C_s} + \frac{(j_1 + j_2) l}{i\omega C_m} &= 0 \qquad (8) \\ i\omega\mu_0 H_2 F_2 S - \sigma_s j_2 l + \frac{j_2 l}{i\omega C_s} + \frac{(j_1 + j_2) l}{i\omega C_m} &= 0 \qquad (9) \end{aligned}$$

Using Equation (3), we can first calculate j_1 and j_2 from Equations (8) and (9), and then the effective permeability that was defined in [1]. We obtain:

$$\mu_{eff} = \frac{B_{ave}}{\mu_0 H_3} = \frac{H_0}{H_0 - F_1 j_1 - F_2 j_2} = 1 - \frac{(\omega\mu_0 S)^2 F_2 F_1 (F_1 + F_2) - \mu_0 S\left[(F_1^2 + F_2^2)\frac{1}{C_s} + (F_1 - F_2)^2 \frac{l}{C_m}\right] + iA(\sigma)}{(\omega\mu_0 S)^2 F_1 F_2 - \mu_0 S(F_1 + F_2)(\frac{l}{C_s} + \frac{l}{C_m}) + \frac{1}{\omega^2}\frac{l}{C_s}(\frac{l}{C_s} + \frac{2l}{C_m}) - B(\sigma) + iC(\sigma)} \qquad (10)$$

where

$$A(\sigma) = \omega\mu_0 S(F_1^2 + F_2^2)\sigma_s l$$

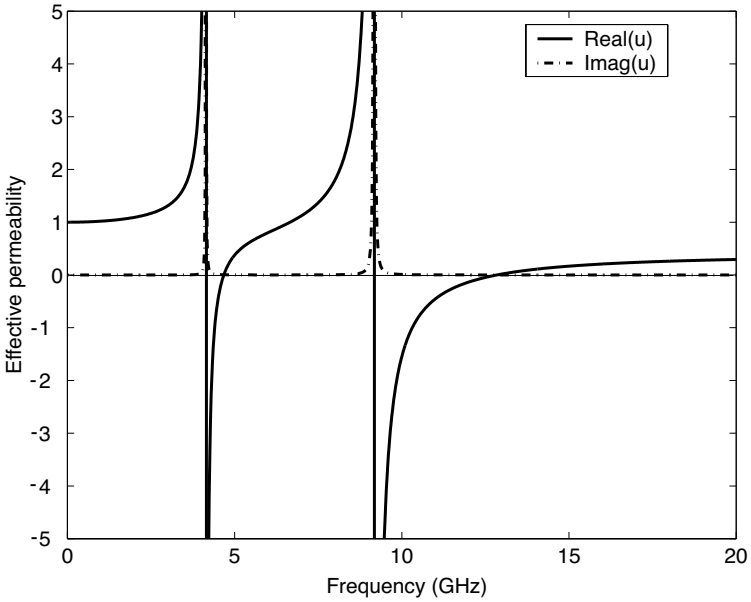

Figure 2. Effective permeability for the S-SRR structure in the case of $F_1 = 0.45$ and $F_2 = 0.15$.

$$\begin{aligned} B(\sigma) &= (\sigma_s l)^2 \\ C(\sigma) &= \left[\omega\mu_0 S(F_1+F_2) - \frac{2}{\omega}\left(\frac{l}{C_s}+\frac{l}{C_m}\right)\right]\sigma_s l \end{aligned} \tag{11}$$

is important to realize that in general, if $F_1 \neq F_2$, Equation (10) has two resonant frequencies:

$$\omega_{m0}^{(1)} = \sqrt{\frac{(m+1)(n+1)+\sqrt{(m-1)^2(n^2+2n)+(m+1)^2}}{2mn}\frac{l}{\mu_0 S F_2 C_s}} \tag{12}$$

$$\omega_{m0}^{(2)} = \sqrt{\frac{(m+1)(n+1)-\sqrt{(m-1)^2(n^2+2n)+(m+1)^2}}{2mn}\frac{l}{\mu_0 S F_2 C_s}} \tag{13}$$

where $m = \frac{F_1}{F_2}$ and $n = \frac{C_m}{C_s}$. Therefore, there will be two frequency bands of negative permeability associated with the two resonant frequencies. This is illustrated in Fig. 2, in which

$$h = 4 \times 10^{-3}\,\mathrm{m}$$

$$\begin{aligned} w &= 7.5 \times 10^{-3}\,\mathrm{m} \\ c &= 0.5 \times 10^{-3}\,\mathrm{m} \\ d &= 0.5 \times 10^{-3}\,\mathrm{m} \\ \sigma_s &= 0.5\,\Omega \\ a &= 10 \times 10^{-3}\,\mathrm{m} \\ b &= 5 \times 10^{-3}\,\mathrm{m} \\ l &= 1 \times 10^{-3}\,\mathrm{m} \\ F_1 &= 0.45 \\ F_2 &= 0.15 \end{aligned} \tag{14}$$

With these parameters, the two resonant frequecies are found to be: $f_{m0}^{(1)} = 9.17 \times 10^9\,\mathrm{Hz}$ and $f_{m0}^{(2)} = 4.14 \times 10^9\,\mathrm{Hz}$. If we take the fringe effects of the capacitances into account, then the newly calculated resonant frequency will be in good agreement with the experimental results. In addition to the double magnetic resonance, we shall also show hereafter that the S-shaped resonator also exhibits an electrical plasma behavior which overlaps with the two magnetic resonances found previously. Therefore, in the case of $F_1 \neq F_2$ considered here, the structure exhibits left-handed properties over two frequency bands.

For the special case where $F_1 = F_2 = F$, Equation (10) becomes

$$\mu_{eff} = 1 - \frac{2F + iD(\sigma)}{1 - \dfrac{1}{\omega^2 \mu_0 FS}\left(\dfrac{l}{C_s} + \dfrac{2l}{C_m}\right) - E(\sigma) + iG(\sigma)} \tag{15}$$

where

$$\begin{aligned} X &= (\omega \mu_0 FS)^2 \left(1 - \frac{1}{\omega \mu_0 FS}\frac{l}{C_s}\right) \\ D(\sigma) &= A(\sigma)/X \\ E(\sigma) &= B(\sigma)/X \\ G(\sigma) &= C(\sigma)/X \end{aligned} \tag{16}$$

The magnetic resonance frequency is given by

$$\omega_{m0} = \sqrt{\frac{1}{\mu_0 FS}\left(\frac{l}{C_s} + \frac{2l}{C_m}\right)} \tag{17}$$

and the magnetic plasma frequency is given by

$$\omega_{mp} = \sqrt{\frac{1}{\mu_0 FS(1-2F)}\left(\frac{l}{C_s} + \frac{2l}{C_m}\right)} = \omega_{m0}\sqrt{\frac{1}{1-2F}} \tag{18}$$

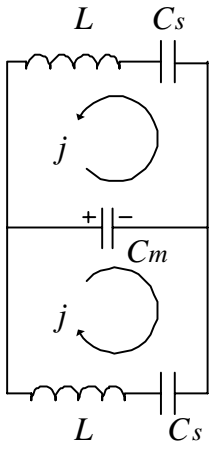

Figure 3. Equivalent circuit of the S-SRR structure.

As predicted in [7], if we take the inductance per unit length in the y direction of each half ring (L) to be given by the area enclosed by each ring: $L = \mu_0 FS/l$, and the capacitances to be C_s, C_m, respectively, then the structure can be treated as an equivalent circuit, as shown in Fig. 3. Using simple circuit theory, we can directly find the resonant frequency of the circuit to be

$$\omega_{m0} = \sqrt{\frac{1}{L\dfrac{1}{\dfrac{1}{C_s}+\dfrac{1}{C_m/2}}}} = \sqrt{\frac{l}{\mu_0 FS}\left(\frac{1}{C_s}+\frac{2}{C_m}\right)} \tag{19}$$

which agrees with (17). Fig. 4 illustrates the effective permeability when the parameters of the structure are those of Equation (14) but with $F_1 = F_2 = F = 0.3$.

As it has been mentioned earlier, in addition to the negative permeability response, the proposed S-SRR also exhibits a negative permittivity response within the same frequency range [6]. The electrical properties of the S-SSR as shown in Fig. 5(c) are in fact very similar to those of an array of cut rods as depicted in Fig. 5(a). The generic form of the effective permittivity for the rods array has been shown to be [8]

$$\varepsilon_{eff} = 1 - \frac{\omega_{ep}^2 - \omega_{e0}^2}{\omega^2 - \omega_{e0}^2 + i\gamma\omega}. \tag{20}$$

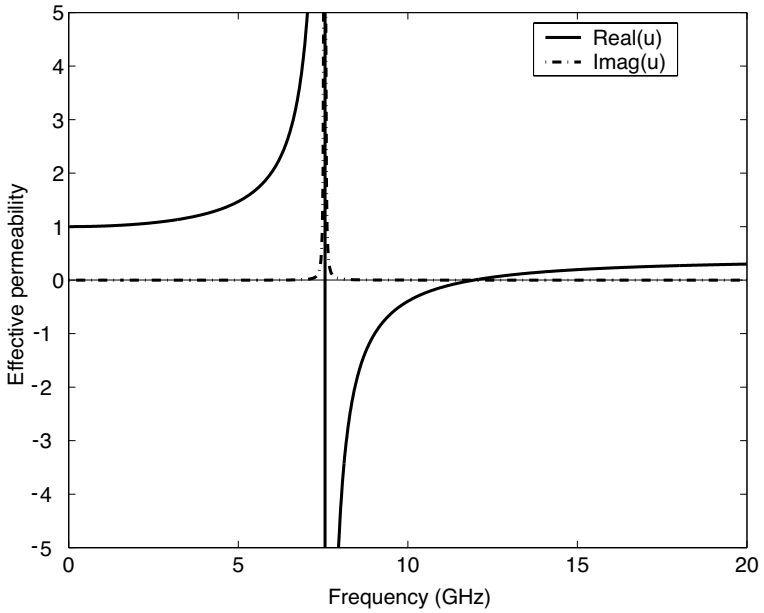

Figure 4. Effective permeability for the S-SRR structure in the case of $F_1 = F_2 = F = 0.3$.

where ω_{e0} is the electric resonant frequency introduced by the interruption in the rods and is determined by the inductance of the wire strips L_e and the capacitance C_e of the interruption [9]. It is important to notice that the 'S' metallic strip array has a lower electric resonant frequency than that of the cut rods array so that we can adjust the parameters of our geometry to control the electric resonance. In fact, we shall show that it is possible to lower it down to the frequencies where the magnetic response is observed. First, we can lower ω_{e0} by enlarging the capacitance of the breaks, as shown in Fig. 5(b), where two horizontal lines are introduced in each break to enlarge the surface area of the capacitance, and thus the value of C_e. Fig. 6 presents the simulation results of the effective permittivity for several different configurations of rods array corresponding to different length of the horizontal line in Fig. 5(b). The results were obtained from the computation of the reflection and transmission coefficients for waves normally incident on a slab of such structure [10, 11], followed by the application of a proper retrieval algorithm [12]. Second, by bending the vertical rods and creating the 'S' pattern as shown in Fig. 5(c), the structure still behaves like a plasma, with ω_{e0} and ω_{ep} further lowered

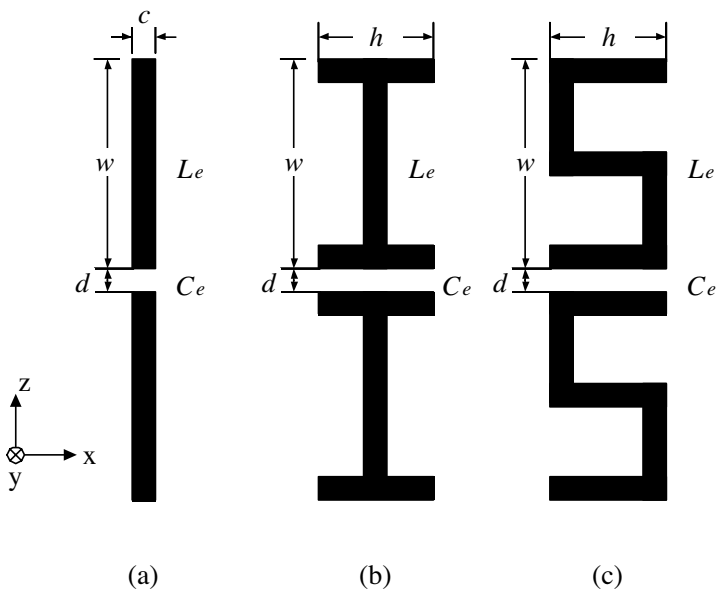

Figure 5. Two unit cells of a periodic arrayed structure (a) a broken rods array, (b) a capacitance-enlarged rods array, (c) a 'S'-shaped rods array.

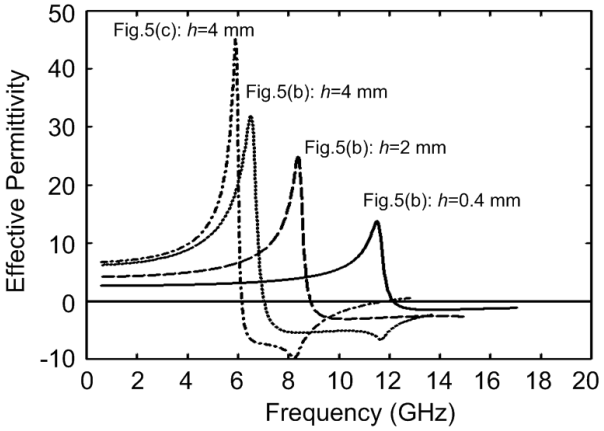

Figure 6. The real part of the effective permittivity measured for some configurations in Fig. 5. The other parameters of the structure is: $w = 9.6\,\text{mm}$, $d = 0.4\,\text{mm}$, $c = 0.4\,\text{mm}$ and the dimensions of a periodic unit cell are $a = 10\,\text{mm}$ in the z direction, $b = 5\,\text{mm}$ in the x direction, and $l = 2.5\,\text{mm}$ in the y direction.

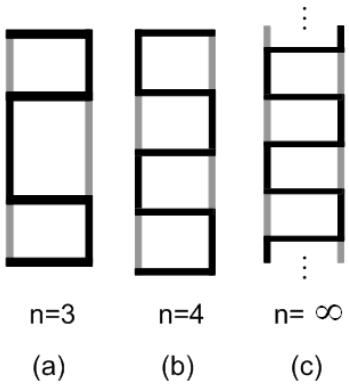

Figure 7. Some ES-SRR structures with each periodic unit cell contains n rings (top view).

by the extra inductance of the greater length of the wire [13]. The simulation result of the effective permittivity for the 'S' structure in Fig. 5(c) is also shown in Fig. 6.

Hence, we can conclude that in the S-SRR structure, each 'S' metallic strip exhibits an electric plasma-like behavior, and the two opposite placed 'S' metallic strips exhibit a magnetic plasma-like behavior. We can also make several S-SRRs connected with each other, as shown in Fig. 7, to further lower the electric resonant frequency ω_{e0} as desired. As the number n of rings in each unit cell of such an extended S-SRR (ES-SRR) structure increases, the analytical expression of the current in the loops becomes increasingly complicated to obtain. However, if n is large enough, or theoretically infinite like shown in Fig. 7(c), and if the unit cell is periodic in the z direction, it is still easy to get the magnetic properties of the structure. For example, if the unit cell has a period of 2 rings in the z direction, then we have only two variables of currents to solve for, as shown in Fig. 8.

The total electromotive force (emf) around the two loops in one periodic unit can be calculated from

$$\begin{aligned} \text{Loop 1}: \ emf_1 &= -\frac{\partial}{\partial t}(\mu_0 H_1 F_1 S) \\ &= \sigma_{s1} I_1 + \frac{1}{C_1}\int (I_1 + I_2)dt + \frac{1}{C_2}\int (I_1 + I_2)dt \quad (21) \\ \text{Loop 2}: \ emf_2 &= -\frac{\partial}{\partial t}(\mu_0 H_2 F_2 S) \\ &= \sigma_{s2} I_2 + \frac{1}{C_1}\int (I_1 + I_2)dt + \frac{1}{C_2}\int (I_1 + I_2)dt \quad (22) \end{aligned}$$

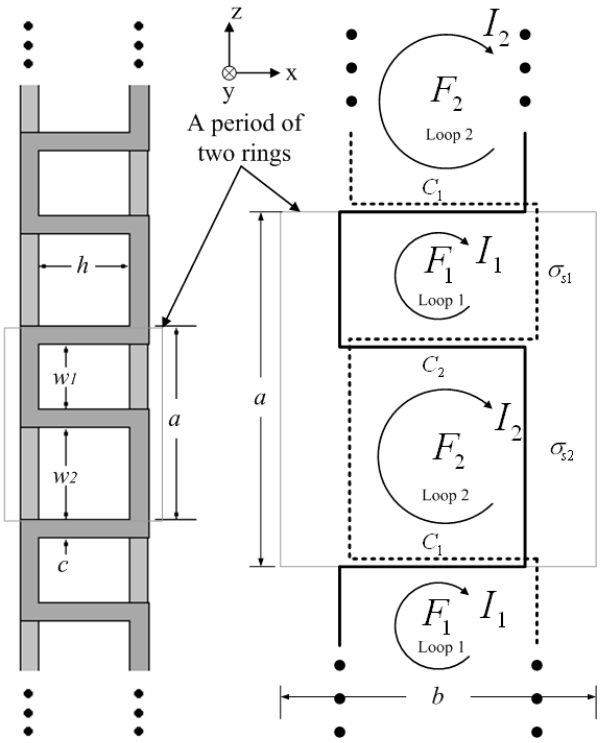

Figure 8. The ES-SRR structure with a period of 2 rings in z direction and its analytical model.

where C_1, C_2 are the capacitances of the two pair of metallic strips, respectively, and σ_{s1}, σ_{s2} are the resistances in each loop, as shown in Fig. 8. Using a similar procedure to that of a standard S-SRR, we can calculate the effective permeability of the ES-SRR structure as:

$$\mu_{eff} = 1 - \frac{A_1 + i\sigma_{s1}l^*A_2 + i\sigma_{s2}l^*A_3}{B_1 + i\sigma_{s1}l^*B_2 + i\sigma_{s2}l^*B_3 - \sigma_{s1}l\sigma_{s2}l} \tag{23}$$

where

$$A_1 = (\mu_0 S)^2 F_1 F_2 \left[\omega^2(F_1 + F_2) - \left(\frac{l}{C_1} + \frac{l}{C_2}\right)\frac{(F_1 - F_2)^2}{(\mu_0 S)F_2 F_1}\right]$$

$$B_1 = (\mu_0 S)^2 F_1 F_2 \left[\omega^2 - \left(\frac{l}{C_1} + \frac{l}{C_2}\right)\frac{(F_1 + F_2)}{(\mu_0 S)F_1 F_2}\right]$$

$$\begin{aligned} A_2 &= \frac{\mu_0 S F_2}{\omega}(\omega^2 F_2) \\ B_2 &= \frac{\mu_0 S F_2}{\omega}\left[\omega^2 - \frac{1}{\mu_0 S F_2}\left(\frac{l}{C_1}+\frac{l}{C_2}\right)\right] \\ A_3 &= \frac{\mu_0 S F_1}{\omega}(\omega^2 F_1) \\ B_3 &= \frac{\mu_0 S F_1}{\omega}\left[\omega^2 - \frac{1}{\mu_0 S F_1}\left(\frac{l}{C_1}+\frac{l}{C_2}\right)\right] \end{aligned} \tag{24}$$

The magnetic resonance frequency is

$$\omega_{m0} = \sqrt{\left(\frac{l}{C_1}+\frac{l}{C_2}\right)\frac{(F_1+F_2)}{(\mu_0 S)F_1 F_2}} \tag{25}$$

and the magnetic plasma frequency is

$$\begin{aligned} \omega_{mp} &= \sqrt{\left(\frac{l}{C_1}+\frac{l}{C_2}\right)\frac{(F_1+F_2)-(F_1-F_2)^2}{(\mu_0 S)F_1 F_2(1-F_1-F_2)}} \\ &= \omega_{m0}\sqrt{\frac{(F_1+F_2)-(F_1-F_2)^2}{(1-F_1-F_2)(F_1+F_2)}} \end{aligned} \tag{26}$$

Using the following values:

$$\begin{aligned} h &= 3\times 10^{-3}\,\mathrm{m} \\ w1 &= 3\times 10^{-3}\,\mathrm{m} \\ w2 &= 5\times 10^{-3}\,\mathrm{m} \\ c &= 0.5\times 10^{-3}\,\mathrm{m} \\ d &= 0.5\times 10^{-3}\,\mathrm{m} \\ a &= 9\times 10^{-3}\,\mathrm{m} \\ b &= 5\times 10^{-3}\,\mathrm{m} \\ l &= 1\times 10^{-3}\,\mathrm{m} \\ \sigma_{s1} &= 0.5\,\Omega \\ \sigma_{s2} &= 0.5\,\Omega \end{aligned} \tag{27}$$

the calculated effective permeability is shown in Fig. 9.

In this structure, we can find that the metallic strips maintain the electrical continuity, which indicates that the electrical resonant frequency is $\omega_{e0} = 0$. Therefore, the lower limit of the frequency band corresponding to the negative permittivity is pushed from a non-zero value to a zero value, and therefore, the frequency band of negative

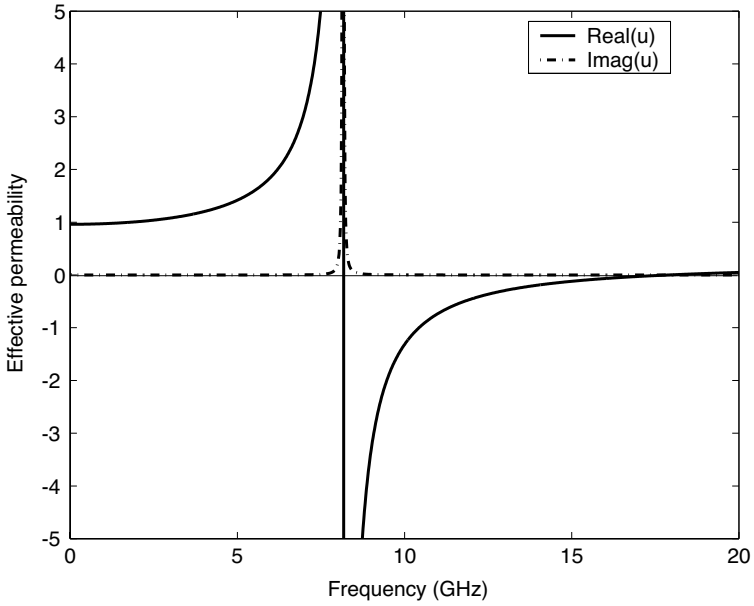

Figure 9. Effective permeability for the ES-SRR structure.

permittivity is enlarged. Also, we see from Equation (26) that when the value of $F_1 + F_2 = F$ is unchanged (i.e., only the ratio of F_1/F_2 is modified), only the case corresponding to $F_1 = F_2 = F/2$ yields the widest frequency band of negative permeability represented by $\omega_{mp}/\omega_{m0} = \sqrt{\frac{1}{1-F}}$.

We can also deduce from Equation (23) two other special cases. The first happens when $\mathrm{Re}(\sigma_{s1}) \gg 1$, for which Equation (23) becomes

$$\mu_{eff} = 1 - \frac{A_2}{B_2 + i\sigma_{s2}l} = 1 - \frac{F_2}{1 - \dfrac{1}{\omega^2\mu_0 S F_2}\left(\dfrac{1}{C_1} + \dfrac{l}{C_2}\right) + i\dfrac{\sigma_{s2}l}{\omega\mu_0 S F_2}} \tag{28}$$

Equation (29) exhibits a similar form as the result of the SRR proposed in [1]. In general, σ_{s1} and σ_{s2} are complex numbers and $\mathrm{Re}(\sigma_{s1}) \gg 1$ indicates that part of the ES-SRR ring is made of insulator material, as shown in Fig. 10(a). Therefore, the ES-SRR structure is simplified to be a periodic structure of SRR (Fig. 10(b)) with a resonant frequency of $\omega_{m0} = \sqrt{\frac{1}{\mu_0 S F_2}\left(\frac{l}{C_1} + \frac{l}{C_2}\right)}$ and a plasma frequency of $\omega_{mp} = \omega_{m0}\sqrt{\frac{1}{1-F_2}}$.

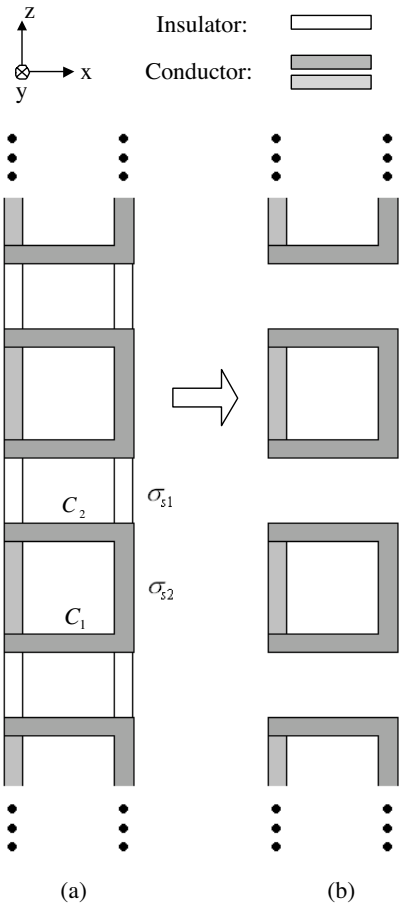

Figure 10. The ES-SRR structure in (a) is simplified into the split ring structure in (b) in the case of $\mathrm{Re}(\sigma_{s1}) \gg 1$.

The second special case happens when $\mathrm{Re}(\sigma_{s2}) \gg 1$. In this case, Equation (23) becomes

$$\mu_{eff} = 1 - \frac{A_3}{B_3 + i\sigma_{s1}l} = 1 - \frac{F_1}{1 - \frac{1}{\omega^2\mu_0 SF_1}\left(\frac{1}{C_1} + \frac{l}{C_2}\right) + i\frac{\sigma_{s1}l}{\omega\mu_0 SF_1}} \tag{29}$$

The resonant frequency is $\omega_{m0} = \sqrt{\frac{1}{\mu_0 SF_1}\left(\frac{l}{C_1} + \frac{l}{C_2}\right)}$ and the plasma frequency is $\omega_{mp} = \omega_{m0}\sqrt{\frac{1}{1-F_1}}$.

3. CONCLUSION

In conclusion, we have theoretically calculated the effective permeability of an S-shaped SRR structure and other several extended S-shaped SRR structures. We concluded that in these 'S'-characterized structures, each S-shaped branch of the metallic strip exhibits an electric plasma-like behavior, and the two opposite placed 'S' metallic strips exhibit a magnetic plasma behavior at certain frequency bands. We find that the electric resonant frequency of the S-SRRs is very low and could be further lowered by connecting a series of such S-SRRs together, to generate the ES-SRR structures. Thus, the frequency band of negative permittivity could be tuned to overlap with the frequency band of negative permeability to realize a metamaterial exhibiting left-handed properties.

ACKNOWLEDGMENT

This work was supported by the Chinese National Science Foundation under Contract No. 60371010.

REFERENCES

1. Pendry, J. B., A. J. Holden, D. J. Robbins, and W. J. Stewart, "Magnetism from conductors and enhanced nonlinear phenomena," *IEEE Trans. Microw. Theory Tech.,* Vol. 47, 2075–2084, 1999.
2. Shelby, R. A., D. R. Smith, and S. Schultz, "Experimental verification of a negative index of refraction," *Science,* Vol. 292, 77–79, 2001.
3. Marqués, R., F. Medina, and R. Rafii-El-Idrissi, "Role of bianisotropy in negative permeability and left-handed metamaterials," *Phys. Rev. B.,* Vol. 65, 144440:1–6, 2002.
4. O'Brien, S. and J. B. Pendry, "Magnetic activity at infrared frequencies in structured metallic photonic crystals," *J. Phys: Condens. Matter,* Vol. 14, 6383–6394, 2002.
5. Grzegorczyk, T. M., C. D. Moss, J. Lu, X. Chen, J. P. Pacheco Jr., and J. A. Kong, "Properties of left-handed metamaterials: transmission, backward phase, negative refraction, and focusing," submitted to *MTT*, 2005.
6. Chen, H., L. Ran, J. Huangfu, X. Zhang, K. Chen, T. M. Grzegorczyk, and J. A. Kong, "Left-handed material composed of only *S*-shaped resonators," submitted, 2004.

7. Veselago, V. G., "The electrodynamics of substances with simultaneously negative values of μ and ε," *Sov. Phys. Usp.,* Vol. 10, 509–514, 1968.
8. Pendry, J. B., A. J. Holden, W. J. Stewart, and I. Youngs, "Extremely low frequency plasmons in metallic mesostructures," *Phys. Rev. Lett.,* Vol. 76, 4773–4776, 1996.
9. Sievenpiper, D. F., E. Yablonovitch, J. N. Winn, S. Fan, P. R. Villeneuve, and J. D. Joannopoulos, "3D metallo-dielectric photonic crystals with strong capacitive coupling between metallic islands," *Phys. Rev. Lett.,* Vol. 80, 2829–2832, 1998.
10. Kong, J. A., "Electromagnetic waves in stratified negative isotropic media," *Progress in Electromagnetics Research,* PIER 35, 1–52, EMW Publishing, Massachusetts, 2002.
11. Smith, D. R., S. Schultz, P. Markoš, and C. M. Soukoulis, "Determination of effective permittivity and permeability of metamaterials from reflection and transmission coefficients," *Phys. Rev. B.,* Vol. 65, 195104:1–5, 2002.
12. Chen, X., T. M. Grzegorczyk, B.-I. Wu, J. P. Pacheco Jr., and J. A. Kong, "Improved method to retrieve the constitutive effective parameters of metamaterials," *Phys. Rev. E*, Vol. 70, No. 016608, 1–7, 2004.
13. Pendry, J. B., A. J. Holden, D. J. Robbins, and W. J. Stewart, "Low frequency plasmons in thin-wire structures," *J. Phys. C.,* Vol. 10, 4785–4808, 1998.

Hong Sheng Chen was born in Zhejiang, China, in 1979. He received the B.S. degree in information science and electrical engineering department from Zhejiang University, China, in 2000. He is currently working toward the Ph.D. degree at Zhejiang University. His current research interests include the application of the left-handed material, design wide-band low-loss metamaterial structures and numerical studies on electromagnetic properties of the metamaterial.

Li Xin Ran was born in P. R. China in 1968. He received the Bachelar, Master and Ph.D. degrees from the Department of Information and Electronic Engineering of Zhejiang University in 1991, 1994 and 1997, respectively. He is currently an associate professor of Zhejiang University. His research interests involve the microwave circuits and chaos, left-handed materials, and high-speed digital circuits.

Jiang Tao Huangfu was born in Henan, China, in 1978. He received the B.S. degree in information science and electrical engineering department from Zhejiang University, China, in 1999. He is currently working toward the Ph.D. degree at Zhejiang University. His current

research interests include the left-handed material and the wireless communication.

Xian Min Zhang was born in Zhejiang, China, in 1965. He received his B.S. and Ph.D. degrees in physical electronics and optoelectronics from Zhejiang University, China, in 1987 and 1992, respectively. He was appointed as an associate professor of information and electronic engineering at Zhejiang University in 1994 and full professor in 1999. He is currently the director of the Institute of Electronic Information Technology and System, Zhejiang University. His research interests include left-handed material, fiber optics, and microwave photonics.

Kang Sheng Chen is a professor of information and electronic engineering at Zhejiang University. From 1992 to 1996, he is the director of the information and electronic engineering department, Zhejiang University. From 1996 to 1999, he is the director of the personal office, Zhejiang University. His research interest is in the area of signal integrity, left-handed material, microwave and optical waveguide technology. He has published two books over 100 refereed articles.

Tomasz M. Grzegorczyk received his Ph.D. thesis from the Laboratoire d'Electromagnétisme et d'Acoustique (LEMA), Ecole Polytecnique Federale de Lausanne (Swiss Federal Institute of Technology, Lausanne) in December 2000. His research activities concerned the modeling of millimeter and submillimeter structures using numerical methods, as well as their technological realizations with the use of micromachining techniques. In January 2001, he joined the Research Laboratory of Electronics (RLE), Massachusetts Institute of Technology (MIT), USA, where he is now a research scientist. His research interests involve the study of wave propagation in complex media including left-handed metamaterials, the polarimetric study of ocean and forest, electromagnetic induction from spheroidal object for unexploded ordnances modeling, waveguide and antenna design, and wave propagation over rough terrains.

Jin Au Kong is a Professor of Electrical Engineering at the Massachusetts Institute of Technology. His research interest is in the area of electromagnetic wave theory and applications. He has published eight books, including Electromagnetic Wave Theory by Wiley Interscience, over 400 refereed articles and book chapters, and supervised over 120 theses. He is editor-in-chief of the Journal of Electromagnetic Waves and Applications, chief editor of the book series Progress in Electromagnetics Research, and editor of the Wiley Series in remote sensing.